EBF1 promotes triple-negative breast cancer progression by surveillance of the HIF1α pathway

Zhaoping Qiu[a,b,1], Weijie Guo[a,b,1], Bo Dong[a,b], Yu Wang[a,b], Pan Deng[c] [ID], Chi Wang[b], Jinpeng Liu[b], Qing Zhang[d] [ID], Rudolf Grosschedl[e], Zhiyong Yu[f], Jiong Deng[g], and Yadi Wu[a,b,2]

Early B cell factor 1 (EBF1) is a transcriptional factor with a variety of roles in cell differentiation and metabolism. However, the functional roles of EBF1 in tumorigenesis remain elusive. Here, we demonstrate that EBF1 is highly expressed in triple-negative breast cancer (TNBC). Furthermore, EBF1 has a pivotal role in the tumorigenicity and progression of TNBC. Moreover, we found that depletion of EBF1 induces extensive cell mitophagy and inhibits tumor growth. Genome-wide mapping of the EBF1 transcriptional regulatory network revealed that EBF1 drives TNBC tumorigenicity by assembling a transcriptional complex with HIF1α that fine-tunes the expression of HIF1α targets via suppression of p300 activity. EBF1 therefore holds HIF1α activity in check to avert extensive mitophagy-induced cell death. Our findings reveal a key function for EBF1 as a master regulator of mitochondria homeostasis in TNBC and indicate that targeting this pathway may offer alternative treatment strategies for this aggressive subtype of breast cancer.

EBF1 | HIF1α | mitophagy | homeostasis | TNBC

Triple-negative breast cancer (TNBC), which lacks ERα, PR, and HER2 expression, is an aggressive disease noted for the development of recurrent, distant metastases and short survival times, particularly in young women (1). The absence of effective targeted therapies and the poor response of TNBC to standard chemotherapy regimens often results in a rapid, fatal outcome.

Early B cell factor 1 (EBF1) was first discovered in early B cells and is one of the key factors in B cell differentiation (2). EBF1 plays important roles in developmental processes, including cell fate decisions, cell differentiation, and cell migration (3). In addition to regulating embryonic neural development and the adult nervous system, EBF1 is expressed at high levels in adipocytes and functions as a key integrator of signal transduction, inflammation, and metabolism (4–6). Notably, EBF1 knockout mice are hypoglycemic and have an increased metabolic rate and increased energy expenditure (7). EBF1 also plays a role in malignant transformation. EBF1 levels are relevant in leukemia (8). Recently, it has been reported that EBF1 contributes to cancer progression by negatively regulating the p53 signaling pathway or modulating telomerase reverse transcriptase expression (9, 10). However, the molecular defect for hypoglycemia in EBF1-deficient mice and the functional role of EBF1 in tumorigenesis remain unclear.

Intriguingly, one of the defining features of TNBC is the increased expression of a large battery of genes that are regulated by HIF1α (11, 12). HIF1 acts as a networking hub to coordinate activities of multiple signaling molecules that influence tumorigenesis (13). However, extensive and prolonged HIF1α activity leads to distinct pathologic responses in many tissues (14, 15). In addition, although the HIF1α-induced glycolytic switch is an important acute adaptive response for cancer growth, chronic and sustained activation of this switch is rather detrimental (16). Importantly, HIF1α, but not HIF2α, is constitutively hyperactivated in TNBC even under a normoxic environment (17), which suggests that coordinated positive and negative regulatory mechanisms control HIF1α activity to ensure that this stress response is tightly regulated under normal nutrient conditions. For example, XBP1 and STAT3 promote TNBC by interaction with HIF1α via the recruitment of RNA polymerase II (Pol II) (18, 19). However, the surveillance system that negatively modulates HIF1α activity to limit the extent of this HIF1α-mediated response in TNBC remains unknown.

Mitochondria, the main energy "powerhouse of the cell," play essential roles in fundamental cellular processes (20). Mitochondrial homeostasis is controlled by balancing mitochondrial biogenesis and mitophagy (21). Mitophagy is a highly specific quality control process which eliminates dysfunctional mitochondria and promotes mitochondrial turnover through the autophagosome–lysosome system (22). HIF1α is a central

regulator of metabolism that allows rapid adaptation to the hypoxic conditions with induction of mitophagy that promotes cancer cell survival (23). However, mitophagy can be a double-edged sword. Excessive or prolonged mitophagy eventually leads to cell death (24), indicating the need for a rigorous control of the extent of this process. In a teleological sense, as cellular stress and altered metabolism persist as a result of HIF1α hyperactivation through oxygen-independent mechanisms in TNBC (17, 25), mitophagy is initiated and persistently activated. However, excessive or persistent activation of HIF1α results in a bioenergetic imbalance and promotes the demise of cancer cells (26). The manner by which TNBC cells overcome this lethal outcome to maintain mitochondrial homeostasis remains elusive.

Here, we found EBF1 deficiency causes severe mitophagy, triggering a switch in glucose metabolism toward glycolysis. We also demonstrated that EBF1 interacts directly with the HIF1α, which then inhibits transactivation of HIF1α target genes by suppression of p300 activity. Our results suggested that EBF1 functions as a master surveillance system for metabolic homeostasis by suppressing HIF1α activity, which, if interrupted, contributes to extensive mitophagy and promotes cell death in TNBC. Our results sufficiently addressed the mechanism used by TNBC cells to fine-tune highly activated HIF1α-induced metabolic homeostasis to promote cell survival and avert cell death.

Results

EBF1 Is Highly Expressed in TNBC. We interrogated the Cancer Cell Line Encyclopedia (CCLE) breast cancer cell line database in search of the molecular factors that might be aberrantly expressed in TNBC and found that EBF1 was highly expressed in TNBC/basal-like breast cancer (BLBC) cell lines (*SI Appendix*, Fig. S1A and B). Immunohistochemical (IHC) analyses of tissue microarrays (TMAs) from breast tumor specimens of different subtypes confirmed that EBF1 expression negatively correlated with ERα expression and was highly expressed in TNBC tumors (Fig. 1A and B). Importantly, EBF1 expression significantly increased with disease progression (Fig. 1C). To examine whether these clinical findings were represented in breast cancer cell lines in vitro, we analyzed a panel of 13 breast cancer cell lines including ER+, HER2+, TNBC, and one nontumorigenic mammary epithelial cell line, MCF 10A. Reverse transcriptase-real time quantitative PCR (RT-qPCR) analysis revealed that *EBF1* expression was markedly higher in TNBC cells, with little expression in ER+ and HER2+ cell lines as compared with MCF 10A (Fig. 1D). Consistent with this, Western blot analysis showed that EBF1 was higher in TNBC cells, completely absent in ER+ cells (Fig. 1E). However, we did not find high expression of EBF1 in clear cell renal cell carcinoma cells with constitutive HIF1α expression (*SI Appendix*, Fig. S1C). Finally, we found that the expression of EBF1 is highly associated with poor survival in breast cancer patients, particular in TNBC (Fig. 1F and G). Collectively, these data demonstrate high expression of EBF1 in the TNBC subtype and implicate this expression with tumor progression.

EBF1 Silencing Blocks TNBC Cell Growth and Invasiveness. To study the role of EBF1 in TNBC, we knocked down EBF1 expression with two independent short hairpin RNA (shRNA) constructs in two TNBC cell lines (Fig. 2A). EBF1 silencing impaired soft agar colony-forming ability and changed cell morphology to a rounded shape in three-dimensional culture, which indicates that EBF1 regulates TNBC anchorage-independent growth (Fig. 2B and *SI Appendix*, Fig. S2A). Depletion of EBF1

also impaired invasiveness (Fig. 2C and *SI Appendix*, Fig. S2B). To extend this assessment of the critical role of EBF1 in regulating cancer stem cell (CSC)–like properties in human breast cancer, we examined tumorsphere formation in EBF1-knockdown clones. We found that EBF1 knockdown greatly reduced the number of tumorspheres (Fig. 2D). To further interrogate the role of EBF1 on CSC properties, we treated cells with doxorubicin. While tumor cell growth was inhibited with doxorubicin treatment, EBF1-deficient cells were more sensitive to treatment (*SI Appendix*, Fig. S2C). We also found that EBF1 ablation sensitized metformin treatment. To rule out a possible death effect from the generation of EBF1-knockdown cells, we produced a doxycycline (Dox)-inducible construct of EBF1 shRNA or control shRNA in MDA-MB-436 cells. Treatment with Dox for 3 d achieved almost complete EBF1 knockdown and was associated with cell growth inhibition within 8 d (*SI Appendix*, Fig. S2D and E). Loss of EBF1 also significantly reduced the colony formation (*SI Appendix*, Fig. S2F). We next used an orthotopic xenograft mouse model with these inducible cells. Tumor growth was significantly inhibited by EBF1 shRNA (Fig. 2E and *SI Appendix*, Fig. S2G). Consistently, the cell proliferation (Ki-67) was reduced while apoptosis (Cleaved-Caspase 3) was markedly increased, accompanied by significant loss of EBF1 (Fig. 2 F and G). To study the role of EBF1 in TNBC progression, we generated EBF1 mammary gland-specific null mice with Cre-keratin 14 (K14). The human K14 gene promoter, which is expressed in the basal epithelium of the mammary gland, is a well-recognized mammary gland promoter (27). We crossed K14^Cre^EBF1^Flox/Flox^ mice with MMTV-Wnt1 mice, a well-established mouse model that closely mimics human breast cancers with basal-like phenotypes and is useful for studying human BLBC (28–30). As previously reported, palpable mammary tumors were detected at 6 to 7 mo of age in female Wnt1; K14^Cre^; EBF1^WT^ mice (28). EBF1 silencing significantly increased MMTV-Wnt1 mice survival (Fig. 2H). Collectively, our data establish a critical role of EBF1 in TNBC progression.

EBF1 Deletion Elicits Extensive Mitophagy. We observed an increase in highly vacuolated cells with EBF1 knockdown compared to control cells. Our observation of intracellular vesiculation and growth inhibition is consistent with autophagy. Therefore, subsequent experiments assessed if autophagy was induced by EBF1 ablation. First, to confirm that the EBF1 deficiency-induced cytoplasmic vacuolation death was distinct from apoptosis and necroptosis, we treated EBF1 shRNA cells with 1) z-VAD-FMK, an inhibitor of caspases and apoptosis; 2) necrostatin-1 (Nec-1), an inhibitor of RIPK1 kinase-mediated necroptosis; 3) 3-methyladenine (3-MA), an inhibitor of class III PI3K activity and early autophagosome formation; and 4) chloroquine (CQ), an inhibitor of late autophagosome formation. Neither z-VAD, Nec-1, nor CQ rescued EBF1 knockdown-induced cell death as measured by trypan blue exclusion (*SI Appendix*, Fig. S3A). In contrast, only 3-MA rescued cell death. Second, we observed a clear increase in autophagic vacuoles labeled with the GFP-LC3 fusion protein (a widely accepted marker of autophagy) in EBF1-shRNA cells compared to control cells. Again, 3-MA treatment decreased autophagic vacuoles (*SI Appendix*, Fig. S3B). To further confirm that cell death was induced by autophagy, we knocked down autophagy-related 7 (ATG7) in EBF1-deficient cells. We found that blockade of this autophagic machinery hampered cell death induced by EBF1 deficiency and blocked the increase of LC3-II induced by EBF1 ablation (*SI Appendix*, Fig. S3C). Third, EBF1 silencing dramatically increased autophagosome
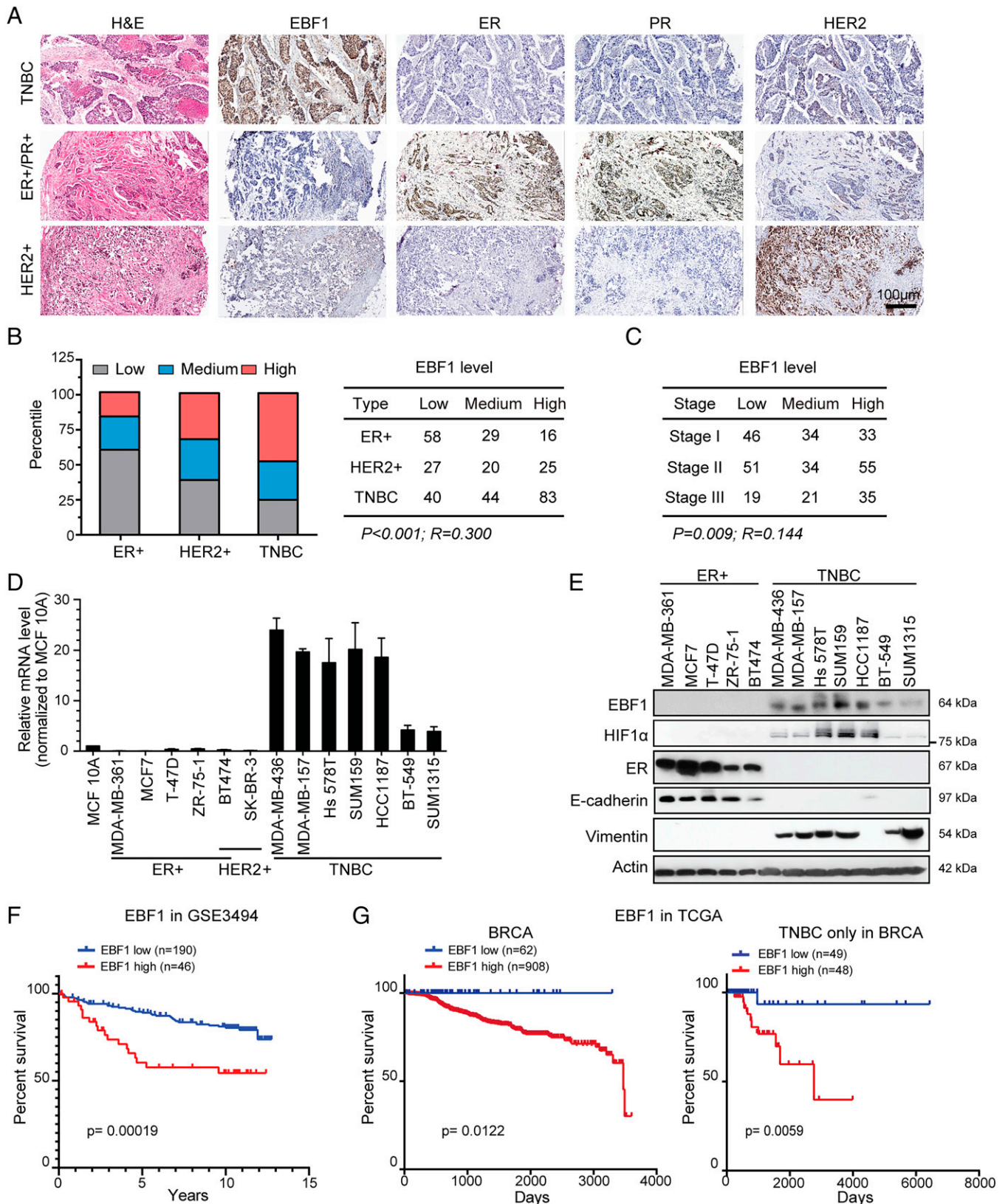
Fig. 1. EBF1 is significantly increased in TNBC. (*A*) Human breast cancer tissue array was stained by hematoxylin/eosin (H&E) and immunohistochemistry for EBF1, ER, PR, and HER2. (Scale bar: 100 μm.) (*B* and *C*) Quantification of EBF1 staining from *A* by cancer type (*B*) and disease stage (*C*). (*D*) RT-qPCR analysis of EBF1 expression in a panel of breast cancer cell lines. (*E*) Expression of the indicated proteins was determined by Western blot using the breast cancer cell lines. Molecular mass markers are indicated on the right in kilodaltons. (*F*) The association of EBF1 expression with survival was assessed in GSE3494 datasets by Kaplan–Meier survival analysis. (*G*) The association of EBF1 expression with survival was assessed in the Cancer Genome Atlas (TCGA) datasets by Kaplan–Meier survival analysis. (*Left*) Breast invasive carcinoma (BRCA); (*Right*) TNBC only in TCGA dataset.

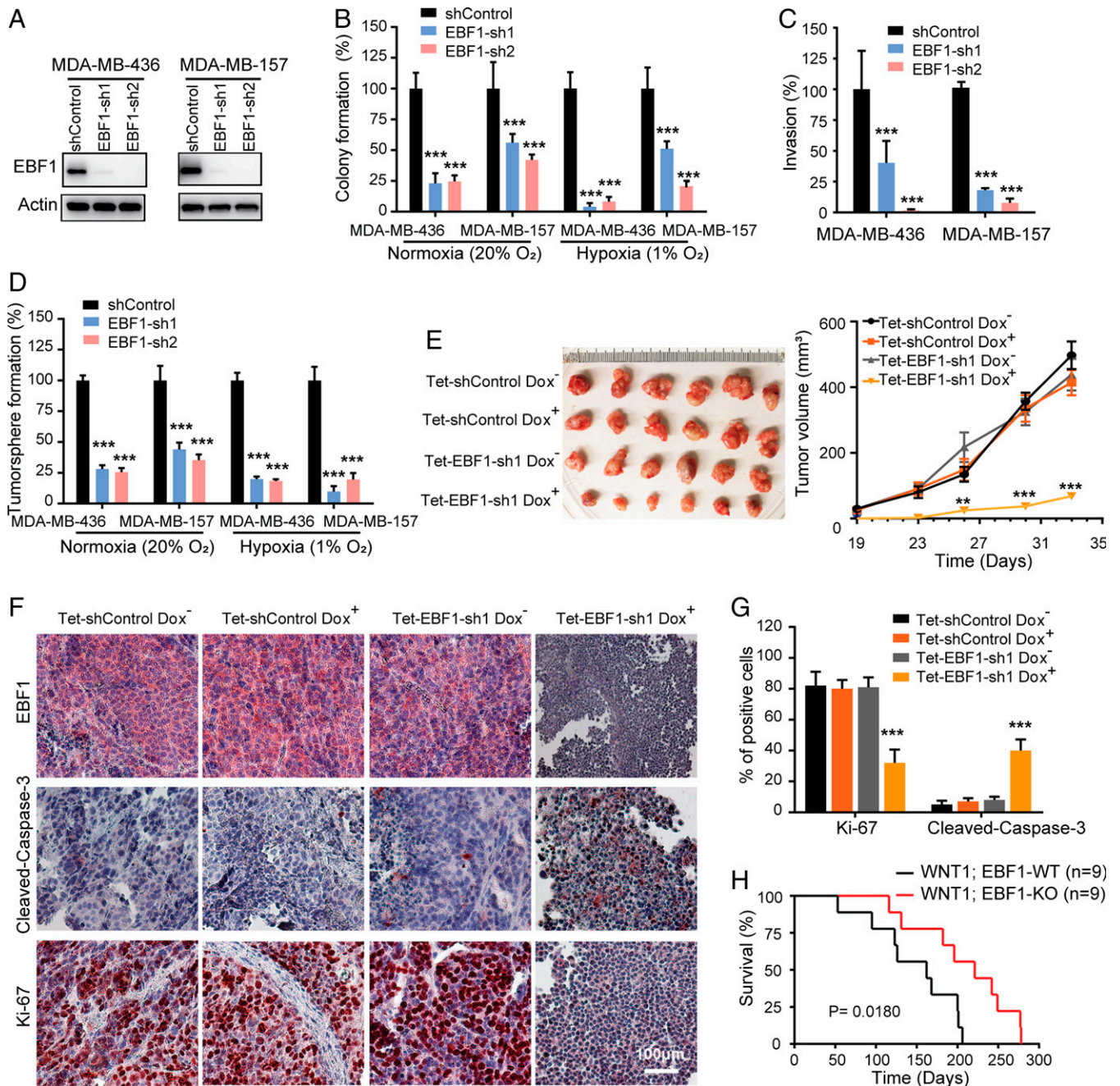**Fig. 2.** EBF1 silencing blocks TNBC cell growth and invasiveness. (*A*) The validation of shRNA-mediated EBF1 knockdown in MDA-MB-436 and MDA-MB-157 cells transduced with nontargeting shRNA control (shControl) or two EBF1 shRNA by immunoblot. (*B*) Soft agar colony formation from shControl and EBF1-silenced cells. (*C*) Graphic representation of cell invasiveness by shControl and EBF1-silenced cells. (*D*) Graphic representation of tumorsphere-formation from shControl and EBF1-silenced cells. (*E*) Tumor growth of MDA-MB-436 cells stably transduced with Dox-inducible shRNA control (Tet-shControl) or EBF1 shRNA with or without Dox treatment. (*F*) IHC staining images for EBF1, Cleaved-Caspase-3, Ki-67 in tumor sections from *E*. (Scale bar: 100 μm.) (*G*) Quantification of cell proliferation and apoptosis in tumor sections from *F*. (*H*) Survival curve of Wnt1; K14Cre; EBF1^{WT} and Wnt1; K14^{Cre}; EBF1$^{f/f}$ mice with tumor size as endpoint. Error bars represent SEM; **$P < 0.01$, ***$P < 0.001$.

formation (*SI Appendix,* Fig. S3*D*). Fourth, EBF1-shRNA cells showed a marked increase in the amount of LC3-II using anti-LC3 in four TNBC cell lines (*SI Appendix,* Fig. S3*E*). Consistently, a specific increase in the levels of LC3-II protein was observed in EBF1 CRISPR knockout cells with two different guided RNAs (*SI Appendix,* Fig. S3*F*). To rule out a nonspecific effect, we expressed the EBF1-shRNA–resistant construct (EBF1-shR) in EBF1 shRNA knockdown cells. Ectopic expression of EBF1 with this construct restored BNIP3 and LC3 expressions, strongly arguing that ablation of EBF1 specifically induced autophagy (*SI Appendix,* Fig. S3*G*). Fifth, Balfilomycin

A1 (Baf A) induced accumulation of LC3-II, which implies a high level of basal autophagy (*SI Appendix,* Fig. S3*H*). More importantly, the elevated levels of LC3-II in the EBF1 shRNA cells showed an additional increase in the presence of Baf A, arguing strongly for an augmentation of autophagosome formation rather than reduced autophagosome–lysosome fusion. Finally, EBF1 knockdown markedly increased autophagy-related genes (*SI Appendix,* Fig. S3*I*).

Because of the cross-talk among autophagy/mitophagy, cell metabolism, and cell death pathways, we wanted to investigate whether the EBF1 deficiency-induced autophagy is in fact

mitophagy. We discovered that mitochondria were depolarized and fragmented in EBF1-deficient cells. In addition, the increased GFP-LC3 extensively colocalized with mitochondria in EBF1-ablated cells (Fig. 3*A* and *SI Appendix*, Fig. S4*A*). Mitochondrial abundance was also estimated by measuring the mitochondrial DNA (mtDNA) over nuclear DNA (nuDNA) ratio. There was a trend to have significantly lower mtDNA/nuDNA in EBF1-ablated cells (*SI Appendix*, Fig. S4*B*). Since loss of mitochondrial membrane potential ($\Delta\psi$m) is a signal of mitophagy (31, 32), we measured the integrity of the mitochondrial membrane by Mito-Shift analysis using tetramethylrhodamine ethyl ester (TMRE) and JC-1. EBF1 knockdown cells exhibited reduced TMRE staining (Fig. 3*B*). An increased number of "unhealthy" green-labeled low-membrane-potential mitochondria was observed in EBF1 knockdown cells compared to the control cells (Fig. 3*C* and *D*). We also applied a more quantitative and sensitive mitophagy assay: mitochondria-targeted mKeima (mt-mKeima) fluorescence-activated cell sorting (FACS) to detect functional mitophagy (33). We observed a substantial fluorescent shift in EBF1 knockdown cells (Fig. 3*E* and *F*). Consistent with this, confocal imaging analysis revealed that knockdown of EBF1 increased the number of mKeima-positive dots (*SI Appendix*, Fig. S4*C*). Transmission electron microscopy revealed that mitochondria showed extensively degenerative changes with loss of cristae membranes, matrix swelling, and even destruction of the outer membranes in EBF1-deficient cells (Fig. 3*G*). To determine whether EBF1 regulates mitochondrial degradation, we used LysoTracker. A fluorescent confocal analysis showed significant colocalization between mitochondria and lysosomes in EBF1-knockdown cells while lysosomes and mitochondria were separate in the control cell group (*SI Appendix*, Fig. S4*D*). In addition, more mitophagy-positive dots were observed in EBF1-knockdown cells, which indicates that mitophagy was activated in EBF1-knockdown cells. Taken together, our data strongly demonstrated that depletion of EBF1 leads to extensive mitophagy in TNBC cells.

Depletion of EBF1 Leads to Mitophagy-Induced Metabolism. Because EBF1 is a key metabolic regulator (5, 7) and because mitophagy triggers metabolic reprogramming and is tightly associated with mitochondrial energy status (34, 35), we investigated the energy status of EBF1-deficient cells. EBF1 inhibition increased glucose uptake and lactate secretion as well as NADPH levels (Fig. 4*A* and *B* and *SI Appendix*, Fig. S5*A*). Enhanced glycolysis directly correlates with stimulation of mitophagy (36, 37). Using Seahorse extracellular flux analyses we measured the extracellular acidification rate (ECAR) to examine glycolysis. EBF1 knockdown cells exhibited an increase in ECAR compared to control cells (Fig. 4*C* and *SI Appendix*, Fig. S5*B*). To assess glycolytic flux, we performed isotopomer distribution analysis using [U-^{13}C]glucose as the tracer. We observed a significant increase of glycolysis and N-acetylglucosamin (GlcNAC) metabolism with a decrease of TCA cycle activity (Fig. 4*D* and *E*). Furthermore, EBF1-depleted cells dramatically increased acetyl-coenzyme A (CoA) levels and PPP activity (Fig. 4*F* and *SI Appendix*, Fig. S5*C*). Pan-metabolomic analyses revealed a marked decrease of glutamate, glutamine, glutathione, and glutathione disulfide (Fig. 4*G*). Consistent with this, a set of glycolytic genes was dramatically increased in EBF1-deficient cells (*SI Appendix*, Fig. S5*D*).

Reactive oxygen species (ROS) play an important role in mitochondrial homeostasis. However, EBF1 deficiency had no effect on the total cell oxidative stress and the mitochondrial ROS production using the DCFH-DA and MitoSOX staining methods, respectively (*SI Appendix*, Fig. S5*E* and *F*). In all, these data

suggest EBF1 reduces glycolytic flux and reshapes glucose metabolism in TNBC cells (Fig. 4*H*).

EBF1 Functions as a Corepressor of HIF1α. To identify the molecular mechanism of the extensive mitophagy induced by EBF1 loss, we performed genome-wide RNA sequencing (RNA-seq) in MDA-MB-436 and MDA-MB-157 cells infected with EBF1 shRNA. Reactome pathway analysis of the differentially expressed genes revealed "Asparagine N-linked glycosylation" and several metabolism-related signaling pathways; mitochondrial translation, mitophagy, and glucose metabolism were among the pathways most significantly affected by EBF1 (Fig. 5*A*). These latter findings are consistent with our earlier observations that EBF1 loss affected mitochondria (Fig. 3). Most importantly, "Cellular response to hypoxia" signaling pathways were the second-most affected group, indicating that EBF1 impacts the hypoxia pathway. Moreover, Gene Set Enrichment Analysis (GSEA) revealed that the EBF1 gene expression profile was negatively associated with the hallmark "hypoxia" (*SI Appendix*, Fig. S6*A*). In contrast, loss of EBF1 up-regulated a set of hypoxia hallmark genes including HK2, JMJD6, and PGK1 (*SI Appendix*, Fig. S6*B*). Interestingly, GSEA also demonstrated that loss of EBF1-induced changes positively correlated with HIF1 target genes (Fig. 5*B*). These results strongly indicated that loss of EBF1 induces mitophagy through HIF1α. To investigate a mechanistic link between EBF1 expression and HIF1α activity, we first tested the functional relationship between HIF1α and EBF1. EBF1 expression inhibited luciferase activity of the hypoxia response element (HRE) under the normoxic condition (Fig. 5*C*). HIF1α expression increased HRE reporter activity, but this effect was largely mitigated by EBF1 coexpression. In addition, expression of EBF1 dramatically decreased HIF1α-induced HRE reporter activity under CoCl$_2$ treatment or in the hypoxic condition. Conversely, EBF1 depletion by two independent shRNA constructs strongly increased HRE reporter activity under the normoxic and hypoxic conditions (Fig. 5*D*). As expected, loss of HIF1α reduced the HRE reporter activity. Surprisingly, knockdown of HIF1α nearly restored all HRE luciferase activity in EBF1-depleted MDA-MB-157 cells both in the normoxic and hypoxic conditions. These data indicate that EBF1 inhibits HIF1α transcriptional activity in TNBC cells.

EBF1 Interacts with HIF1α and Is a Direct Target of HIF1α. We next sought to determine the mechanism of this inhibition. We first examined whether endogenous EBF1 was a relevant inhibitor of HIF1α expression. *HIF1A* messenger RNA (mRNA) levels were similar in control and EBF1-knockdown MDA-MB-157 and MDA-MB-436 cells (*SI Appendix*, Fig. S6*C*). HIF1α regulation occurs mainly at the levels of protein stability (38). EBF1 knockdown also failed to alter protein levels of HIF1α in these two cell lines (*SI Appendix*, Fig. S6*D*). We then explored the possibility of a physical interaction between HIF1α and EBF1. We coexpressed Flag-HIF1α and Myc-EBF1 into HEK293 cells. Coimmunoprecipitation (co-IP) experiments revealed a physical interaction of HIF1α with EBF1 (Fig. 5*E*). We also detected endogenous protein interaction between HIF1α and EBF1 both in the normoxic and hypoxic conditions (Fig. 5*F*). We did not find any effect of EBF1 on association between HIF1α and HIF1β (*SI Appendix*, Fig. S6*E*). Interestingly, EBF1 also associated with HIF2α (*SI Appendix*, Fig. S6*F*). To map HIF1α binding with the domain of EBF1, we generated two EBF1 constructs: 1) an N-terminal domain which consists of N-terminal (N-term) DNA-binding domain and an Ig-like/plexins/transcription factors (IPT) domain and 2) a C-terminal (C-term) domain including a helix–loop–helix (HLH) dimerization domain and a C-terminal
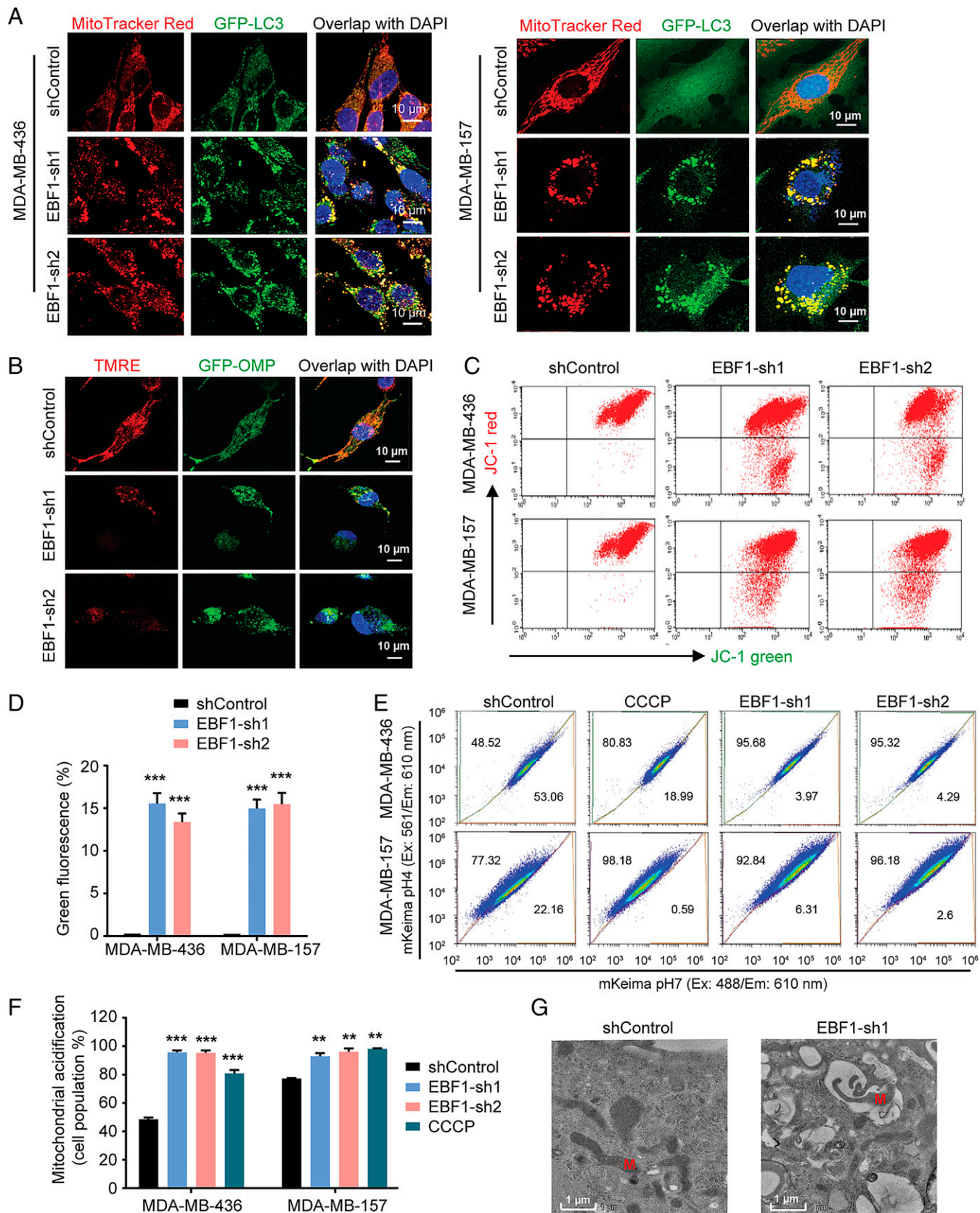
Fig. 3. Loss of EBF1 leads to extensive mitophagy. (*A*) Confocal microscopic analysis of GFP-LC3 and MitoTracker Red in shControl and EBF1-silenced cells. (Scale bars: 10 μm.) (*B*) Confocal microscopic analysis of GFP-mitochondrial outer membrane protein 25 (GFP-OMP) and TMRE staining for membrane potential in shControl and EBF1-silenced cells. (Scale bars: 10 μm.) (*C*) Mitochondrial membrane potential (MMP) of shControl and EBF1-silenced cells was detected by using the JC-1 staining. (*D*) Quantification of MMP in *C*. (*E*) shControl, cells treated with CCCP (carbolyl cyanide chlorophenylhydrazone), or EBF1-silenced cells stably expressing mt-mKeima were subjected to FACS analysis. CCCP was used as a positive control. (*F*) Quantification of mitophagy in *E*. (*G*) Representative electron micrographs of mitochondrial morphology from shControl and EBF1-silenced MDA-MB-157 cells. M (highlighted with red color): mitochondria. (Scale bars: 1 μm.) Error bars represent SEM; **$P < 0.01$, ***$P < 0.001$.
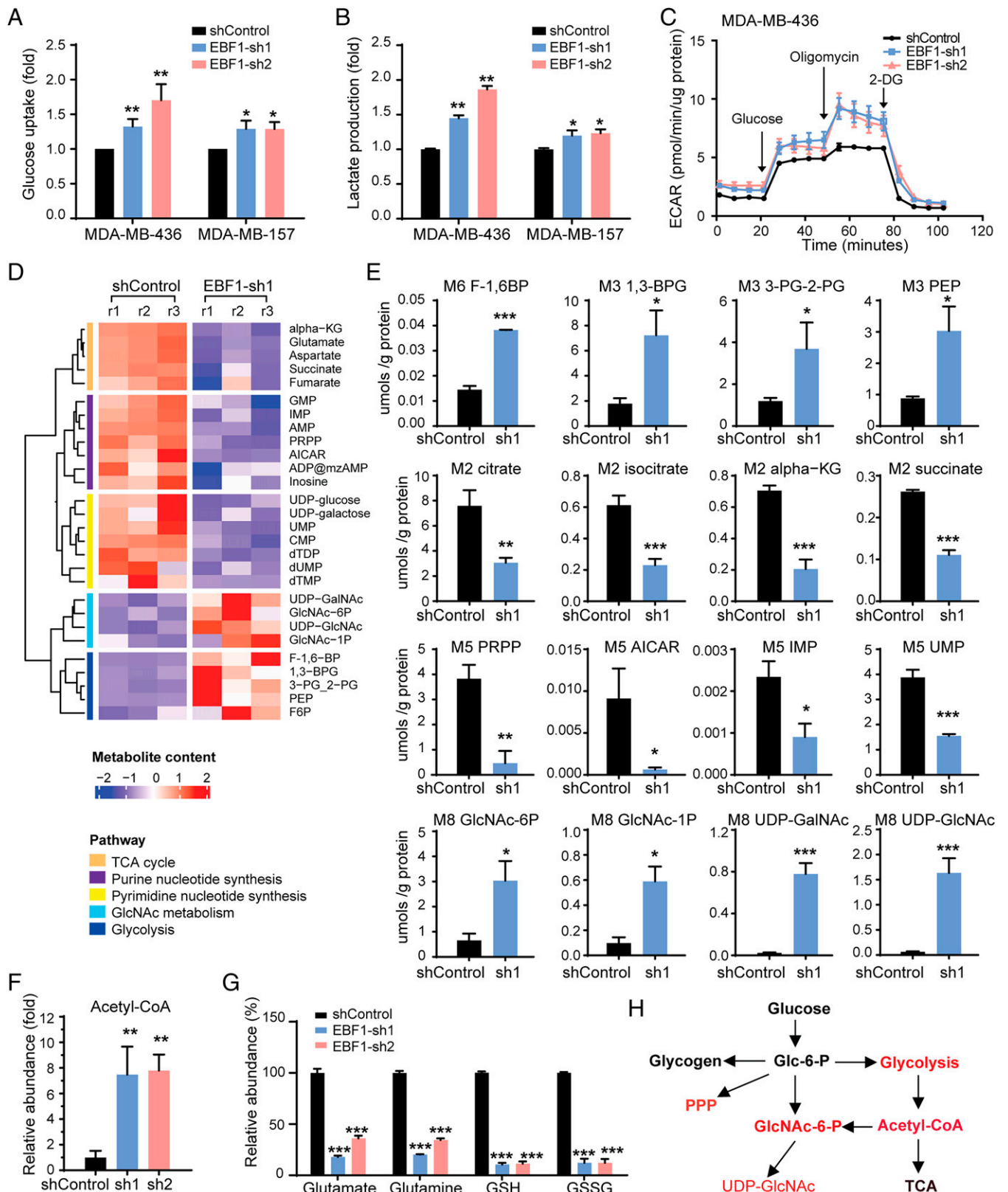
Fig. 4. EBF1 regulates glycolysis. (*A*) Glucose uptake in MDA-MB-436 and MDA-MB-157 cells with or without EBF1 depletion. (*B*) Lactate secretion in MDA-MB-436 and MDA-MB-157 cells with or without EBF1 depletion. (*C*) ECAR was measured in MDA-MB-436 cells with or without EBF1 depletion. (*D*) Heat map with distribution of indicated metabolites in shControl or EBF1-depleted MDA-MB-436 cells by the metabolomics analysis. (*E*) The indicated metabolites were measured by stable isotope-resolved metabolomics (SIRM) in MDA-MB-436 cells with or without EBF1 ablation. (*F*) Acetyl-CoA level in MDA-MB-436 cells with or without EBF1 ablation. (*G*) The indicated metabolites were measured by NMR in MDA-MB-436 cells with or without EBF1 ablation. (*H*) Major steps of glycolysis affected by EBF1 (highlighted with red color). Error bars represent SEM; *$P < 0.05$, **$P < 0.01$, ***$P < 0.001$.

transactivation domain (39). We expressed Myc-tagged wild type (WT), N-term, and C-term constructs of EBF1 and Flag-HIF1α into HEK293 cells. Analysis of IP revealed that only N-term, but not the C-term, of EBF1 is responsible for interaction with Flag-HIF1α (Fig. 5*G*). In vitro GST pull-down assays further confirmed that the N-term of EBF1 was strongly bound to HIF1α
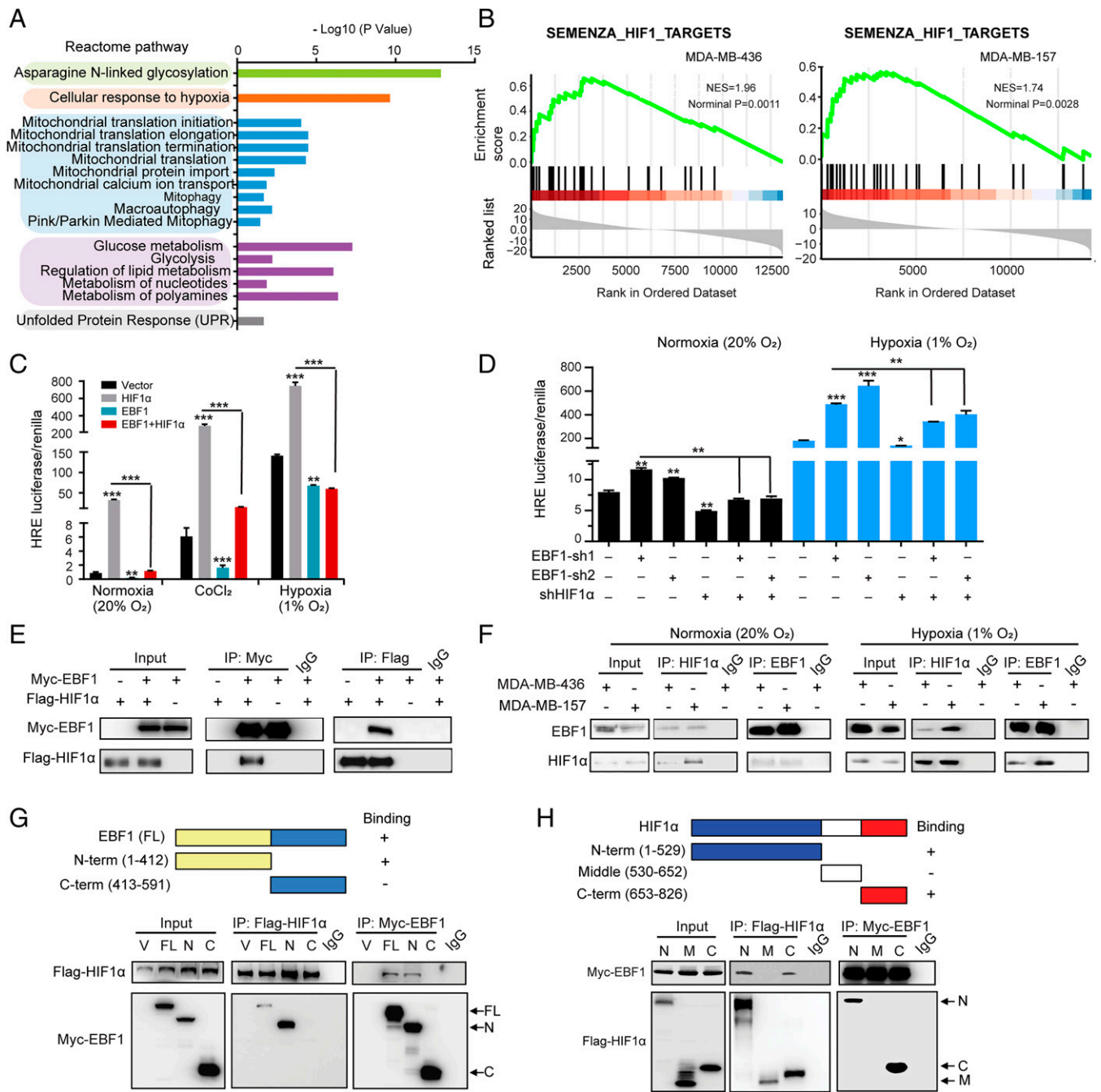
Fig. 5. EBF1 interacts with HIF1α and inhibits HIF1α activity. (*A*) Reactome pathway analysis of the significantly increased pathways in EBF1-depleted cells. (*B*) GSEA enrichment plots for "SEMENZA_HIF1_TARGETS" signature by RNA-seq (EBF1 shRNA versus control shRNA). (*C*) The 3xHRE reporter activity measured in HEK293 cells transfected with indicated constructs. (*D*) The 3xHRE reporter activity measured in MDA-MB-157 cells transfected with indicated constructs. (*E*) Co-IP of exogenous Myc-EBF1 and Flag-HIF1α in HEK293 cells. (*F*) Co-IP of endogenous EBF1 and HIF1α. (*G*) Schematic diagram showing the structure of EBF1 and deletion constructs used (*Upper*). Co-IP of exogenous Flag-HIF1α and Myc-full length (FL) EBF1 or different deletion mutants (*Lower*). V: control vector. (*H*) Schematic diagram showing the structure of HIF1α and deletion constructs used (*Upper*). Co-IP of exogenous Myc-EBF1 and Flag-HIF1α different deletion mutants (*Lower*). Error bars represent SEM; *P < 0.05, **P < 0.01, ***P < 0.001.

(*SI Appendix*, Fig. S6*G*). Consistent with this, only the N-term domain, but not the C-term domain, of EBF1 significantly inhibited HIF1α transcriptional activity (*SI Appendix*, Fig. S6*H*). We then identified the region in HIF1α that associated with EBF1. HIF1α contains a basic HLH/Per-arnt-Sim domain at its N terminus, two transactivation domains (N-TAD and C-TAD) at the C terminus, and an oxygen-dependent degradation domain in the middle portion (40). We observed that both N terminus and C terminus, but not middle-terminus, of HIF1α were responsible for interaction with EBF1 (Fig. 5*H*). EBF1 also interacted with an HIF1α mutant harboring an N803A mutation (*SI Appendix*, Fig. S6*I*). To

determine which domain of HIF1α is responsible for EBF1 inhibition, we replaced the HIF1α DNA-binding domain with a GAL4 DNA-binding domain (GBD) and performed GAL4 transactivation assays. Consistent with the above observations, EBF1 inhibited the transactivity of the full-length HIF1α (GBD) in normoxic and hypoxic conditions (*SI Appendix*, Fig. S6*J*). EBF1 also reduced the transactivation of N-terminal and C-terminal, but not middle, domains of HIF1α. Taken together, our results demonstrated that EBF1 interacts with HIF1α and suppresses HIF1α activity.

Interestingly, we found that the EBF1 protein level was diminished when HIF1α was knocked down under normoxic and

hypoxic conditions (*SI Appendix*, Fig. S7*A*). Moreover, RT-qPCR analysis revealed that mRNA levels of *EBF1* were also decreased in HIF1α-knockdown cells (*SI Appendix*, Fig. S7*B*). Analysis of the human *EBF1* gene sequence revealed two potential HIF1α binding sites. In agreement with this, HIF1α significantly increased *EBF1* promoter activity which contains potential HRE sites (*SI Appendix*, Fig. S7*C*). In contrast, depletion of HIF1α markedly reduced *EBF1* promoter activity (*SI Appendix*, Fig. S7*D*). Our chromatin IP coupled with deep sequencing (ChIP-seq) analysis also revealed the HIF1α binding site (*SI Appendix*, Fig. S7*E*). ChIP-qPCR analysis further confirmed that HIF1α was associated with the *EBF1* promoter (*SI Appendix*, Fig. S7*F*). These results indicated that EBF1 is a direct target of HIF1α.

EBF1 Regulates HIF1α Signaling. To understand the association between EBF1 and HIF1α at the genomic level, we performed ChIP-seq of EBF1 and HIF1α under hypoxic conditions in MDA-MB-157 cells. We then overlapped the EBF1 ChIP-seq with HIF1α ChIP-seq data and found that 895 peaks were commonly regulated by both transcriptional factors (Fig. 6*A*); this represents ∼10% of EBF1 or HIF1α regulated peaks. Hypoxia induced extensive binding of HIF1α to chromatin. Interestingly, EBF1 chromatin binding overlapped with HIF1α binding (*SI Appendix*, Fig. S8*A* and *B*). Motif analysis of EBF1 and HIF1α revealed a statistically significant enrichment, indicating colocalization of HIF1α and EBF1 to the same regulatory elements (Fig. 6*B*). To link these binding events to transcriptional regulation, we performed integrated analysis for ChIP-seq and RNA-seq. First, binding and expression target analysis showed that EBF1 peaks with increased enrichment had significant effects as a gene repressor (*SI Appendix*, Fig. S8*C*). We then identified differently expressed genes with binding peaks for both EBF1 and HIF1α and identified 196 up-regulated genes (15% of total up-regulated genes in EBF1-knockdown cells) (*SI Appendix*, Fig. S8*D*). These up-regulated genes are highly plausible direct targets of HIF1α and EBF1 (Fig. 6*C*). We selected four well-known HIF1α-target genes that were up-regulated and that both HIF1α and EBF1 occupy: Voltage-dependent anion channel 1 (*VDAC1*), Tumor M2-pyruvate kinase (*PKM2*), RUN Domain-Containing Protein 1 (*RUNDC1*), and Jumonji domain-containing 6 (*JMJD6*) (Fig. 6*D*). First, we examined the expression of these genes. RT-qPCR analysis revealed that ablation of EBF1 dramatically increased the expression of these genes (Fig. 6*E* and *SI Appendix*, Fig. S8*E*). We next established that EBF1 and HIF1α cooccupied these targets using ChIP-qPCR (Fig. 6*F* and *SI Appendix*, Fig. S8*F*). Knockdown of endogenous EBF1 significantly increased HIF1α occupancy at the HRE of these genes in hypoxic MDA-MB-157, MDA-MB-436, and Hs 578T cells but not at the nonrelated gene *CDH1*, indicating that EBF1 specifically suppresses HIF1α binding at the HRE of target genes (Fig. 6*G* and *SI Appendix*, Fig. S8*G*). Most importantly, we observed that knockdown of HIF1α restored expression of these genes in EBF1 and HIF1α double-knockdown cells (Fig. 6*H* and *SI Appendix*, Fig. S8*H*). Ablation of HIF1β impaired HIF1α binding on these common target genes (*SI Appendix*, Fig. S8*I* and *J*). However, depletion of EBF1 did not affect the expression of genes bound by HIF1α alone (*SI Appendix*, Fig. S8*K*).

The histone acetyltransferase p300 is a coactivator of HIF1α and is required for full activity of transactivation (41). Interestingly, both HIF1α and EBF1 bind p300, but EBF1 inhibits p300 histone acetyltransferase (HAT) activity (42). To test whether EBF1 and HIF1α can bind to p300 simultaneously, whereby EBF1 interferes in HIF1α/p300-mediated transactivation and p300 HAT activity, we first transfected Myc-EBF1, Flag-HIF1α,

and HA-p300 into HEK293 cells and immunoprecipitated with anti-HA antibody; the binding of EBF1 and HIF1α was found by Myc and Flag antibodies, respectively (*SI Appendix*, Fig. S9*A*). Endogenous co-IP further confirmed the association between HIF1α and EBF1 with p300 in MDA-MB-157 and MDA-MB-436 cells under the hypoxic condition (*SI Appendix*, Fig. S9*B*). To determine whether p300 mediated the interaction between EBF1 and HIF1α, we knocked down p300 and employed co-IP. Loss of p300 had no effect on the interaction between HIF1α and EBF1 (*SI Appendix*, Fig. S9*C*), which indicates that HIF1α interacts with EBF1 directly and that these three proteins form the complex. EBF1 depletion markedly restored (*SI Appendix*, Fig. S9*D*), while EBF1 expression dose-dependently inhibited, p300 induced-HRE luciferase activity (*SI Appendix*, Fig. S9*E*) in both normoxic and hypoxic conditions. To test whether EBF1 represses HIF1α transcriptional activity through p300, we generated an EBF1 mutant construct (291 to 592), which lacks inhibitory activity on p300 (42). As expected, cotransfection of the p300 expression vector did, indeed, enhance HRE promoter activity under both normoxic and hypoxic conditions, but this was suppressed by WT-EBF1. However, the EBF1 mutant abolished the ability to repress HIF1α transcriptional activity (*SI Appendix*, Fig. S9*F*). To further investigate whether EBF1 inhibits p300 HAT activity and impairs full activation of HIF1α target genes, we examined the histone acetylation of H3 at lysine K27 (H3K27ac) at the promoter region of HIF1α-target genes, in control or EBF1 shRNA knockdown cells. ChIP-qPCR analysis revealed that levels of H3K27ac at the *VDAC1*, *PKM2*, *RUNDC1*, and *JMJD6* were significantly increased (*SI Appendix*, Fig. S9*G*). Interestingly, EBF1 knockdown also increased the total cellular H3K27ac and H3K9ac levels (*SI Appendix*, Fig. S9*H*). Expression of shRNA-resistant exogenous EBF1 in EBF1-knockdown cells largely restored the expression levels of H3K9ac and H3K27ac (*SI Appendix*, Fig. S9*I*). Collectively, our findings support the concept that EBF1 is a negative regulator of HIF1α transcriptional activity by specifically interfering with the activity of p300 through inhibition of histone acetylation, an epigenetic modification associated with gene transcription.

Inhibition of HIF1α Rescues the Phenotype in EBF1-Deficient Cells. Because ablation of EBF1 induces extensive mitophagy and EBF1 represses HIF1α signaling, and because HIF1α is critical for mitophagy and extensive mitophagy eventually induced cell death, we thus examined whether knockdown of HIF1α rescued the EBF1 ablation-induced effect in TNBC cells with double-knockdown experiments. Intriguingly, knockdown of HIF1α markedly reduced EBF1-deficiency-induced cell death (*SI Appendix*, Fig. S10 *A* and *B*). Western blot analysis for LC3-II confirmed loss of HIF1α and treatment with the HIF1α inhibitor Bay87-2243 decreased the EBF1 deletion-mediated increase of LC3-II levels (*SI Appendix*, Fig. S10 *C* and *D*). In addition, loss of HIF1α partially blocked EBF1 deficiency-induced mitophagy (*SI Appendix*, Fig. S10*E*). Functionally, ablation of HIF1α restored EBF1 deficiency-induced ECAR, glucose uptake, and lactate levels (*SI Appendix*, Fig. S10 *F*–*H*). Consistent with these functions, ablation of HIF1α restored expression levels of glycolytic genes increased by EBF1 deficiency (*SI Appendix*, Fig. S10*I*). These results strongly suggest the EBF1 deficiency-induced mitophagy is HIF1α-dependent and EBF1 guides HIF1α activity to maintain mitochondrial homeostasis.

The Protein Levels of HIF1α and EBF1 Are Coordinately Overexpressed in TNBC. To further examine the EBF1–HIF1α relationship in human breast cancer, we performed IHC analysis for EBF1 and HIF1α expression in a breast TMA generated by
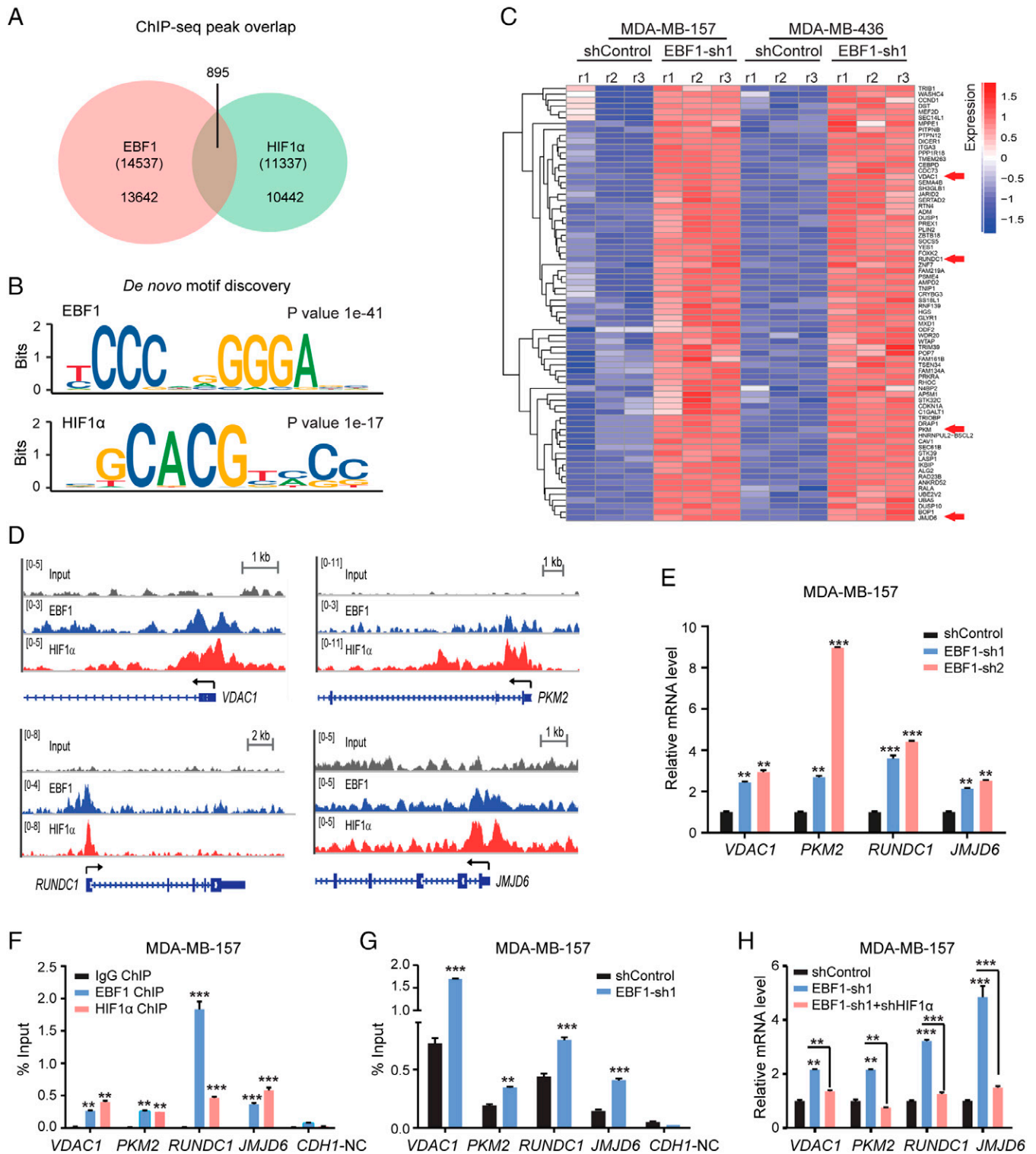
Fig. 6. EBF1 is a coregulator of HIF1α. (*A*) The graphic shows the number of EBF1 ChIP-seq peaks and HIF1α ChIP-seq peaks and extent of overlap between them. Permutation test for 10,000 simulation; $P = 0.0001$. (*B*) Identification of EBF1 and HIFα motif with ChIP-seq dataset in MDA-MB-157 cells. Matrices predicted by the de novo motif-discovery algorithm Seqpos. (*C*) Heat map depicting $\log_2$ fold change of up-regulated differentially expressed genes (DEGs) in shControl or EBF1-depleted MDA-MB-157 cells. Arrows indicate selected genes. (*D*) ChIP-seq distribution for EBF1 and HIF1α at representative gene loci. (*E*) qRT-PCR analysis of genes in shControl or EBF1-depleted MDA-MB-157 cells. (*F*) ChIP-qPCR analysis of the occupancy of indicated genes using EBF1, HIF1α, or immunoglobulin G (IgG) antibody. *CDH1*-NC was used as a negative control distal region. (*G*) ChIP-qPCR analysis of the occupancy of indicated genes using HIF1α antibody in shControl or EBF1-depleted MDA-MB-157 cells. *CDH1*-NC was used as a negative control distal region. (*H*) qRT-PCR analysis of genes in EBF1-knockdown or EBF1+ HIF1α-knockdown MDA-MB-157 cells. Error bars represent SEM; **$P < 0.01$, ***$P < 0.001$.

our cancer center. The TMA contains 342 cases of breast tumor specimens, including 102 ER+, 71 HER2-overexpressing, and 169 TNBC (Fig. 7*A* and *B*). We found the intensity and distribution of HIF1α-positive staining correlated with EBF1 (Fig. 7*A*).

In addition, the expression of HIF1α was positively associated with EBF1 in several breast cancer datasets (*SI Appendix*, Fig. S11*A*). In alignment with this, the EBF1 expression was negatively correlated with HIF1α target genes (*SI Appendix*, Fig. S11*B*).
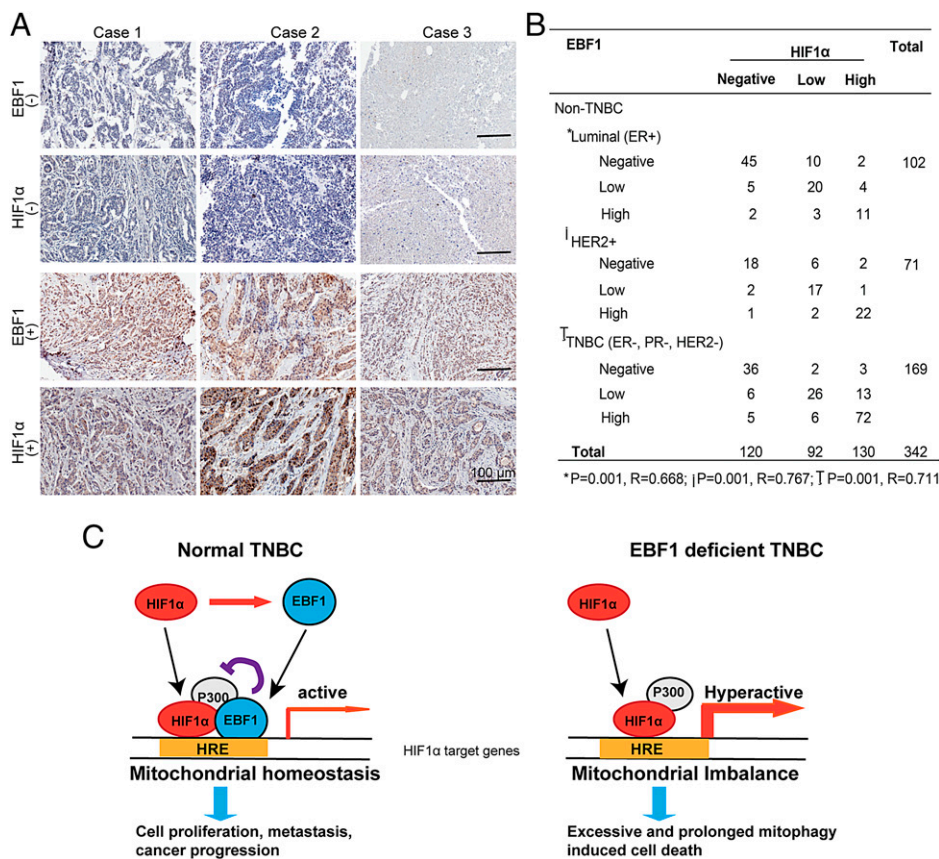
Fig. 7. Expression of EBF1 and HIF1α are positively correlated in breast cancer patients. (*A*) The 342 surgical specimens of breast cancer were immunostained using antibodies against EBF1 and HIF1α. Shown are images with consecutive IHC staining for both EBF1 and HIF1α in six cases of breast tumors (top two rows: three cases of negative staining for both proteins; bottom two rows: three cases for positive staining for both proteins). (Scale bars: 100 μm.) (*B*) Statistical analysis of *A*. (*C*) Schematic model of the mechanism proposed for this study.

B

EBF1	HIF1α			Total
	Negative	Low	High	
Non-TNBC				
*Luminal (ER+)				
Negative	45	10	2	102
Low	5	20	4	
High	2	3	11	
|HER2+				
Negative	18	6	2	71
Low	2	17	1	
High	1	2	22	
†TNBC (ER-, PR-, HER2-)				
Negative	36	2	3	169
Low	6	26	13	
High	5	6	72	
Total	120	92	130	342

*P=0.001, R=0.668; |P=0.001, R=0.767; †P=0.001, R=0.711

Discussion

From this study, we demonstrate that EBF1 interacts with HIF1α and functions as a master surveillance system for metabolic homeostasis that holds active HIF1α in check, to prevent extensive mitophagy and mitochondrial imbalance in TNBC. EBF1 enables TNBC cells to maintain a pool of healthy mitochondria that facilitates the bioenergetic and biosynthetic needs during tumor progression (Fig. 7*C*). Our findings reveal that EBF1 is critical for mitochondria homeostasis. This EBF1-promoted mitochondrial protective activity is particularly important for tumor growth in normoxic conditions. HIF1α-induced mitophagy has dual roles as it maintains tumor cell survival and, paradoxically, cell death. Resolution of this paradox has proved challenging. EBF1 may function as an important surveillance system to sense a panel of mitochondrial content variables and react to metabolic imbalance by fine-tuning mitophagy and reestablishing homeostasis. Loss of EBF1 leads to progressive and unrelenting mitophagy and imbalanced mitochondria which eventually promotes cell death (Fig. 7*C*). Interestingly, our evidence also indicates that EBF1 is a direct target gene of HIF1α (*SI Appendix*, Fig. S7) and that EBF1 resides within a feedback loop such that HIF1α activates EBF1 expression, which then represses HIF1α target genes. This EBF1–HIF1α circuitry is critical as a mitochondrial homeostasis rheostat.

We found that EBF1 had no effect on HIF1α protein stability or mRNA levels but that it did interact with HIF1α and inhibited the activity of HIF1α. Interestingly, EBF1 is one of the top-ranked nonredundant variables that is coincident with HIF1α (43). Both proteins function as transcription factors of stress responses (44). In addition, motif analysis of EBF1 revealed a statistically significant enrichment of both HIF1α and EBF1 (Fig. 6*B*), which indicates frequent colocalization of HIF1α and EBF1 to the same regulatory elements (43). Notably, we found that

silencing HIF1α did not completely rescue the EBF1 deficiency-induced mitophagy and cell death. This finding suggests that there are HIF1α-independent mechanisms. EBF1 has other widespread effects that contribute to TNBC progression.

HIF1α cooperates with a variety of transcription factors along with alternative positive and negative feedback regulators to fine-tune the transcriptional response to hypoxia to favor of diverse biological responses in a context-dependent fashion (45). Because optimal intervention in HIF1α activity does not lie on the extreme side (either all/full activation or all/full inhibition) but rather in a balanced and fine-tuned manipulation (46), we realized that EBF1, as a feedback regulator, selectively regulates a subset of HIF1α target genes. Indeed, based on our RNA-seq and ChIP-seq data, we noticed that only fewer than 10% of HIF1α-target genes were coregulated by EBF1 and HIF1α (Fig. 6 and *SI Appendix*, Fig. S8). For example, VDAC1 is the gatekeeper for the passage of metabolites that converge on the crossroads of metabolism, cell survival pathway, and cell death (47). It is a decisive regulator between mitophagy and apoptosis (48). We found that both EBF1 and HIF1α occupied the *VDAC1* promoter and that EBF1 inhibited while HIF1α increased VDAC1 expression. These two factors counterbalance VDAC1 expression.

Overall, we uncovered a role for EBF1 as a regulator of mitochondria homeostasis by fine-tuning HIF1α transcriptional activity in TNBC. These findings fill a critical gap in our knowledge about the surveillance system of HIF1α activity in metabolic reprogramming. Our results indicate that EBF1 sits at a critical metabolic node, modulating glycolytic metabolism and mitochondria homeostasis through fine-tuning HIF1α activity (Fig. 7*C*). EBF1 deficiency leads to robust metabolic reprogramming, extensive mitophagy, and eventual cell death.

Materials and Methods

The materials used in this study, including cell lines, chemicals, antibodies, and sequences for single-guide RNAs are described in *SI Appendix*. Detailed descriptions of the study methods, including cell culture and transfection, stable cell line generation, TMA, IHC, co-IP, Western blot, GST pull-down assays, RT-qPCR and ChIP-qPCR, and in vitro migration and invasion assays, luciferase reporter and GAL4 transactivation assay, generation of MMTV-Wnt1/EBF1 knockout mice, FACS, tumorsphere-formation assay, colony formation assay, measurement of mitochondrial membrane potential, transmission electron microscopy, metabolic assays, and in vivo tumorigenesis assay are also provided in *SI Appendix*.

Data Availability. CHIP-seq data have been deposited in Gene Expression Omnibus (GEO) (accession no. 195816). All other study data are included in the article and/or *SI Appendix*.

Author affiliations: [a]Department of Pharmacology and Nutritional Science, College of Medicine, The University of Kentucky, Lexington, KY 40506; [b]Markey Cancer Center, College of Medicine, The University of Kentucky, Lexington, KY 40506; [c]Department of Pharmaceutical Sciences, College of Medicine, The University of Kentucky, Lexington, KY 40506; [d]Department of Pathology, University of Texas Southwestern Medical Center, Dallas, TX 75390; [e]Department of Cellular and Molecular Immunology, Max Planck Institute of Immunobiology and Epigenetics, 79108 Freiburg, Germany; [f]Department of Oncology, Shandong Cancer Hospital and Institute, Shandong Academy of Medical Sciences, Shandong First Medical University, Shandong 250117, China; and [g]Key Laboratory of Cell Differentiation and Apoptosis of Chinese Minister of Education, Shanghai Jiao Tong University School of Medicine, Shanghai 200925, China

1. S. Badve *et al.*, Basal-like and triple-negative breast cancers: A critical review with an emphasis on the implications for pathologists and oncologists. *Mod. Pathol.* **24**, 157–167 (2011).
2. S. Boller, R. Grosschedl, The regulatory network of B-cell differentiation: A focused view of early B-cell factor 1 function. *Immunol. Rev.* **261**, 102–115 (2014).
3. D. Liberg, M. Sigvardsson, P. Akerblad, The EBF/Olf/Collier family of transcription factors: Regulators of differentiation in cells originating from all three embryonal germ layers. *Mol. Cell. Biol.* **22**, 8389–8397 (2002).
4. S. S. Wang, R. Y. Tsai, R. R. Reed, The characterization of the Olf-1/EBF-like HLH transcription factor family: Implications in olfactory gene regulation and neuronal development. *J. Neurosci.* **17**, 4149–4158 (1997).
5. M. J. Griffin *et al.*, Early B-cell factor-1 (EBF1) is a key regulator of metabolic and inflammatory signaling pathways in mature adipocytes. *J. Biol. Chem.* **288**, 35925–35939 (2013).
6. H. Gao *et al.*, Early B cell factor 1 regulates adipocyte morphology and lipolysis in white adipose tissue. *Cell Metab.* **19**, 981–992 (2014).
7. J. A. Fretz *et al.*, Altered metabolism and lipodystrophy in the early B-cell factor 1-deficient mouse. *Endocrinology* **151**, 1611–1621 (2010).
8. C. G. Mullighan *et al.*, Genome-wide analysis of genetic alterations in acute lymphoblastic leukaemia. *Nature* **446**, 758–764 (2007).
9. M. Xing *et al.*, Genomic and epigenomic EBF1 alterations modulate TERT expression in gastric cancer. *J. Clin. Invest.* **130**, 3005–3020 (2020).
10. A. Shen *et al.*, EBF1-mediated upregulation of ribosome assembly factor PNO1 contributes to cancer progression by negatively regulating the p53 signaling pathway. *Cancer Res.* **79**, 2257–2270 (2019).
11. C. M. Perou *et al.*, Molecular portraits of human breast tumours. *Nature* **406**, 747–752 (2000).
12. N. Cancer Genome Atlas; Cancer Genome Atlas Network, Comprehensive molecular portraits of human breast tumours. *Nature* **490**, 61–70 (2012).
13. S. Soni, Y. S. Padwad, HIF-1 in cancer therapy: Two decade long story of a transcription factor. *Acta Oncol.* **56**, 503–515 (2017).
14. K. C. Allan *et al.*, Non-canonical targets of HIF1a impair oligodendrocyte progenitor cell function. *Cell Stem Cell* **28**, 257–272.e11 (2021).
15. K. Takubo *et al.*, Regulation of the HIF-1alpha level is essential for hematopoietic stem cells. *Cell Stem Cell* **7**, 391–402 (2010).
16. L. Zhong *et al.*, The histone deacetylase Sirt6 regulates glucose homeostasis via Hif1alpha. *Cell* **140**, 280–293 (2010).
17. K. J. Briggs *et al.*, Paracrine induction of HIF by glutamate in breast cancer: EgIN1 senses cysteine. *Cell* **166**, 126–139 (2016).
18. X. Chen *et al.*, XBP1 promotes triple-negative breast cancer by controlling the HIF1α pathway. *Nature* **508**, 103–107 (2014).
19. M. R. Pawlus, L. Wang, C. J. Hu, STAT3 and HIF1α cooperatively activate HIF1 target genes in MDA-MB-231 and RCC4 cells. *Oncogene* **33**, 1670–1679 (2014).
20. P. Mishra, D. C. Chan, Metabolic regulation of mitochondrial dynamics. *J. Cell Biol.* **212**, 379–387 (2016).
21. C. Ploumi, I. Daskalaki, N. Tavernarakis, Mitochondrial biogenesis and clearance: A balancing act. *FEBS J.* **284**, 183–195 (2017).
22. W. X. Ding, X. M. Yin, Mitophagy: Mechanisms, pathophysiological roles, and analysis. *Biol. Chem.* **393**, 547–564 (2012).
23. N. M. Mazure, J. Pouysségur, Hypoxia-induced autophagy: Cell death or cell survival? *Curr. Opin. Cell Biol.* **22**, 177–180 (2010).
24. D. A. Kubli, A. B. Gustafsson, Mitochondria and mitophagy: The yin and yang of cell death control. *Circ. Res.* **111**, 1208–1221 (2012).
25. A. Lin *et al.*, The LINK-A lncRNA activates normoxic HIF1α signalling in triple-negative breast cancer. *Nat. Cell Biol.* **18**, 213–224 (2016).
26. J. W. Kim, P. Gao, C. V. Dang, Effects of hypoxia on tumor metabolism. *Cancer Metastasis Rev.* **26**, 291–298 (2007).
27. J. Jonkers *et al.*, Synergistic tumor suppressor activity of BRCA2 and p53 in a conditional mouse model for breast cancer. *Nat. Genet.* **29**, 418–425 (2001).
28. X. Liu *et al.*, Somatic loss of BRCA1 and p53 in mice induces mammary tumors with features of human BRCA1-mutated basal-like breast cancer. *Proc. Natl. Acad. Sci. U.S.A.* **104**, 12111–12116 (2007).
29. Y. Li, W. P. Hively, H. E. Varmus, Use of MMTV-Wnt-1 transgenic mice for studying the genetic basis of breast cancer. *Oncogene* **19**, 1002–1009 (2000).
30. J. I. Herschkowitz *et al.*, Identification of conserved gene expression features between murine mammary carcinoma models and human breast tumors. *Genome Biol.* **8**, R76 (2007).
31. J. J. Lemasters, Selective mitochondrial autophagy, or mitophagy, as a targeted defense against oxidative stress, mitochondrial dysfunction, and aging. *Rejuvenation Res.* **8**, 3–5 (2005).
32. G. Twig *et al.*, Fission and selective fusion govern mitochondrial segregation and elimination by autophagy. *EMBO J.* **27**, 433–446 (2008).
33. H. Katayama, T. Kogure, N. Mizushima, T. Yoshimori, A. Miyawaki, A sensitive and quantitative technique for detecting autophagic events based on lysosomal delivery. *Chem. Biol.* **18**, 1042–1052 (2011).
34. S. Melser *et al.*, Rheb regulates mitophagy induced by mitochondrial energetic status. *Cell Metab.* **17**, 719–730 (2013).
35. H. Zhang *et al.*, Mitochondrial autophagy is an HIF-1-dependent adaptive metabolic response to hypoxia. *J. Biol. Chem.* **283**, 10892–10903 (2008).
36. C. H. Eng, R. T. Abraham, The autophagy conundrum in cancer: Influence of tumorigenic metabolic reprogramming. *Oncogene* **30**, 4687–4696 (2011).
37. V. M. Hubbard *et al.*, Macroautophagy regulates energy metabolism during effector T cell activation. *J. Immunol.* **185**, 7349–7357 (2010).
38. W. G. Kaelin, Jr, P. J. Ratcliffe, Oxygen sensing by metazoans: The central role of the HIF hydroxylase pathway. *Mol. Cell* **30**, 393–402 (2008).
39. N. Treiber, T. Treiber, G. Zocher, R. Grosschedl, Structure of an Ebf1:DNA complex reveals unusual DNA recognition and structural homology with Rel proteins. *Genes Dev.* **24**, 2270–2275 (2010).
40. C. J. Schofield, P. J. Ratcliffe, Oxygen sensing by HIF hydroxylases. *Nat. Rev. Mol. Cell Biol.* **5**, 343–354 (2004).
41. Z. Arany *et al.*, An essential role for p300/CBP in the cellular response to hypoxia. *Proc. Natl. Acad. Sci. U.S.A.* **93**, 12969–12973 (1996).
42. F. Zhao, R. McCarrick-Walmsley, P. Akerblad, M. Sigvardsson, T. Kadesch, Inhibition of p300/CBP by early B-cell factor. *Mol. Cell. Biol.* **23**, 3837–3846 (2003).
43. D. Villar *et al.*, Cooperativity of stress-responsive transcription factors in core hypoxia-inducible factor binding regions. *PLoS One* **7**, e45708 (2012).
44. L. Tacchini, D. Fusar-Poli, A. Bernelli-Zazzera, Activation of transcription factors by drugs inducing oxidative stress in rat liver. *Biochem. Pharmacol.* **63**, 139–148 (2002).
45. X. Xia, A. L. Kung, Preferential binding of HIF-1 to transcriptionally active loci determines cell-type specific response to hypoxia. *Genome Biol.* **10**, R113 (2009).
46. A. T. Henze, T. Acker, Feedback regulators of hypoxia-inducible factors and their role in cancer biology. *Cell Cycle* **9**, 2749–2763 (2010).
47. A. K. S. Camara, Y. Zhou, P. C. Wen, E. Tajkhorshid, W. M. Kwok, Mitochondrial VDAC1: A key gatekeeper as potential therapeutic target. *Front. Physiol.* **8**, 460 (2017).
48. S. J. Ham *et al.*, Decision between mitophagy and apoptosis by Parkin via VDAC1 ubiquitination. *Proc. Natl. Acad. Sci. U.S.A.* **117**, 4281–4291 (2020).